PHILOSOPHICAL TRANSACTIONS OF THE ROYAL SOCIETY A MATHEMATICAL, PHYSICAL & ENGINEERING SCIENCES

Thermocline penetration by buoyant plumes

Kevin Speer

Phil. Trans. R. Soc. Lond. A 1997 **355**, 443-458
doi: 10.1098/rsta.1997.0016

Thermocline penetration by buoyant plumes

By Kevin G. Speer

Laboratoire de Physique des Océans IFREMER/CNRS, B.P. 70, 29280 Plouzané, France

Plumes of buoyant fluid rise in a stratified environment until their buoyancy with respect to the environment reverses, they become heavier than their surroundings and gravitational forces bring them to a halt. Obstacles to turbulent plume rise, occur in the form of external stratification and two-component mixing, which changes the buoyancy of the plume. Volcanic eruptions introduce large amounts of heat to the water column, and the question arises as to whether or not such eruptions can drive plumes up to the sea surface, and create a significant sea surface temperature anomaly.

A turbulent plume model is used to estimate the magnitude of an eruption which might be capable of driving a plume across the ocean's thermocline, which poses a substantial barrier to vertical motion—more so, for instance, than the tropopause with respect to atmospheric plumes. The confining effect of Earth's rotation helps to maintain stronger anomalies in the horizontal spreading phase of the motion at the sea surface. Plumes which cannot attain the surface may also have substantial temperature and salinity anomalies if these quantities vary in the the source or water column through which the plume rises and entrains water.

1. Introduction

The effect of marine geothermal sources is mostly hidden from view, occuring for the most part on deep mid-ocean ridges where new crust is formed, or in basins where old crust is sinking into the Earth. Often the sources are thousands of metres deep, and require large institutional efforts merely to access them. While their effect can be dramatic on the deep ocean environment, as they are capable of sustaining life and generating ocean circulation, a whole new class of environmental effects is implied if these geothermal sources should somehow modify significantly the sea surface temperature (SST). Air–sea interaction in the form of heat and moisture fluxes from the ocean to the atmosphere strongly depends on the sea surface temperature, as phenonema ranging from the El Niño-southern oscillation to hurricanes are at least partly controlled by sea surface temperature anomalies of a few degrees Celsius.

Volcanoes can modify the sea surface temperature directly when they happen near the surface, on seamounts, for instance, or when lava from terrestrial eruptions flows into the sea. Large eruptions presumably generate significant SST anomalies, but the direct heat input from magma has to compete with secondary effects such as anomalous winds, ash clouds and aerosols affecting the Sun's energy input and particulates in the surface layer which modify absorption. The physics of this complex surface layer activity clearly involves atmospheric circulation as well as oceanic circulation, and has been studied from the atmospheric perspective especially in terms

Phil. Trans. R. Soc. Lond. A (1997) **355**, 443–458
Printed in Great Britain

of the large-scale influence of aerosol injections on global temperature. The *indirect* heating of the sea surface by seafloor geothermal sources projected to the surface in hydrothermal plumes is considered here. The focus is on the rising and spreading plume generated by the geothermal sources; further interaction of hot plumes with the atmosphere has been suggested, among other things, to be partly responsible for triggering El Niño (Walker 1995) and, in extreme cases, large hurricane-like storms (Emanuel *et al.* 1995).

How strong does the heat source on the seafloor have to be in order to generate a buoyant plume capable of reaching the surface? To answer this question the full water column density (buoyancy) structure, or stratification must be taken into account. Over most of the ocean, away from high latitudes and outside of marginal seas, the stratification can be characterized by a deep, subthermocline density gradient of $-10^{-4}\,\mathrm{kg\,m^{-3}}$ per metre, and a shallow thermocline gradient of $-10^{-2}\,\mathrm{kg\,m^{-3}}$ per metre. Corresponding buoyancy frequencies (N, table 1) are $N = 10^{-3}\,\mathrm{s^{-1}}$ in deep water, and $N = 10^{-2}\,\mathrm{s^{-1}}$ in the thermocline. A turbulent buoyant jet is characterized (see, for example, Turner 1986) by its initial volume flux Q (units: L^3T^{-1}), momentum source M (L^4T^{-2}), and buoyancy source F (L^4T^{-3}). From these quantities, two length scales may be constructed representing the distance to which source geometry and initial momentum influence plume evolution. A 1 MW hydrothermal vent discharging at $1\,\mathrm{ms^{-1}}$ through a 10 cm diameter orifice has, roughly, $Q = 10^{-2}\,\mathrm{m^3\,s^{-1}}$, $M = 10^{-2}\,\mathrm{m^4\,s^{-2}}$, and $F = 10^{-3}\,\mathrm{m^4\,s^{-3}}$; at distances greater than $l_M = M^{3/4}F^{-1/2} = 1\,\mathrm{m}$ and $l_Q = Q^{3/5}F^{-1/5} = 0.3\,\mathrm{m}$ the orifice geometry and momentum source are unimportant and the resulting plume may be characterized by F alone, emanating from a virtual point source about 1 m below the orifice. These distances and orifice size are all small compared to rise height, even for the strong sources to be considered here. (Little *et al.* (1987) provide a detailed discussion of source characteristics for a particular vent site).

From N and F, rising plume scales may be constructed for height H_N, velocity W_N, and buoyancy g'_N:

$$h_N = (F/N^3)^{1/4}, \tag{1.1}$$

$$W_N = (FN)^{1/4}, \tag{1.2}$$

$$g'_N = (FN^5)^{1/4}. \tag{1.3}$$

From the definition of N, the buoyancy jump across the thermocline is N^2H, where H is the vertical thickness scale of the thermocline, roughly 500 m. Setting the plume buoyancy equal to that of the thermocline, $(N^5F)^{1/4} = N^2H$, we find that $F = N^3H^4$. With thermocline values for N and H, $F \sim 10^5\,\mathrm{m^4\,s^{-3}}$ represents the source strength needed to penetrate the thermocline. Up to the base of the thermocline the stratification is weak by comparison and F is approximately conserved in the plume. This source has to operate over a time period of at least one buoyancy period N^{-1} if the plume is to reach the surface; stronger sources for proportionally shorter periods generate thermals with the same penetration scale H.

The associated heat source is approximately $(\rho C_p/g\alpha)F$, or about 10^7 MW, for $\rho = 500\,\mathrm{kg\,m^{-3}}$, $C_p = 6000\,\mathrm{J\,kg^{-1}\,{}^\circ C^{-1}}$ and $\alpha = 3 \times 10^{-3}$ (values relevant to high-temperature seawater). The transfer of this much buoyancy to cooler ambient temperature seawater by conduction at the surface of freezing magma requires a somewhat higher heat source, of order 10^8 MW, mainly because α is smaller at lower temperatures. This source strength is far greater than that from a vent or cluster of vents,

Table 1. *Definition of basic parameters, where T is temperature, S is salinity, ρ is density, ρ_{amb} is the ambient density, ρ_o is a constant reference density and g is gravity*

parameter	symbol	units
Coriolis parameter	f	s^{-1}
buoyancy frequency	$N = \left(-g\dfrac{\partial \rho_{\mathrm{amb}}}{\partial z}\right)^{1/2}$	s^{-1}
buoyancy	$b = -g\dfrac{(\rho - \rho_{\mathrm{amb}})}{\rho_o}$	$\mathrm{m\ s}^{-2}$
reduced gravity	$g' = -b$	$\mathrm{m\ s}^{-2}$
thermal expansion	$\alpha = -\dfrac{1}{\rho}\dfrac{\partial \rho}{\partial T}$	$^{\circ}\mathrm{C}^{-1}$
haline contraction	$\beta = +\dfrac{1}{\rho}\dfrac{\partial \rho}{\partial S}$	10^{-3}
specific heat	C_p	$\mathrm{J\ kg}^{-1}\ ^{\circ}\mathrm{C}^{-1}$
vertical velocity	W	$\mathrm{m\ s}^{-1}$
specific mass transport	Q	$\mathrm{m}^3\ \mathrm{s}^{-1}$
momentum transport	M	$\mathrm{m}^4\ \mathrm{s}^{-2}$
heat flux	H	$\mathrm{W\ m}^{-2}$
excess salt flux	$W(S - S_{\mathrm{amb}})$	$\mathrm{m}\ ^{\circ}/_{\infty}\ \mathrm{s}^{-1}$
heat transport	$\mathcal{H}$	W
salt transport	$\mathcal{S}$	$\mathrm{kg\ s}^{-1}$
buoyancy flux	$B = \dfrac{g\alpha\mathcal{H}}{\rho C_p} + g\beta W(S - S_{\mathrm{amb}})$	$\mathrm{m}^2\ \mathrm{s}^{-3}$
buoyancy transport	$F = \displaystyle\int_{\mathrm{area}} B\,\mathrm{d}A$	$\mathrm{m}^4\ \mathrm{s}^{-3}$

Table 2. *Plume regimes based on order of magnitude values of source strengths $\mathcal{H}$ and F, and associated velocity and transport scales in the flow above the source*

	$\mathcal{H}$ (MW)	F ($\mathrm{m}^4\ \mathrm{s}^{-3}$)	W ($\mathrm{m\ s}^{-1}$)	Q ($\mathrm{m}^3\ \mathrm{s}^{-1}$)
vent	10	10^{-2}	10^{-1}	10^{-2}
mound	10^2	10^{-1}	1	1
megaplume	10^5	10	1	10^2
hyperplume	10^8	10^5	10	10^6

and roughly one thousand times greater than even that thought to be responsible for the largest observed plumes, or megaplumes (Baker *et al.* 1987). For convenience, plumes formed by sources of this magnitude may be termed hyperplumes (table 2).

An immediate question arises concerning the plausibility of supplying this amount of heat by magma outflow and subsequent cooling. A magma supply of roughly $10^4 - 10^5\ \mathrm{m}^3\ \mathrm{s}^{-1}$ appears to be needed to be cooled to ambient temperature, transferring heat to the seawater. A further question about the *mechanism* of this transfer is pertinent, because lava flows tend to cap themselves with an insulating ceramic lid,

and simple scaling with plausible conductivity coefficients suggests that huge areas would be needed if thicknesses more than a few metres or so are built up by the outflow. Thus a turbulent mixing between the magma and seawater, as might occur in explosive eruptions, is necessary to obtain such heat transfer rates. Whether or not these conditions are satisfied by an immense eruption (high pressure at the seafloor would reduce gas expansion) or bollide impact, for instance, is hard to estimate; but heat sources of comparable strength have been documented in the largest terrestrial eruptions (Wilson *et al.* 1978)—though of short duration.

It is assumed here that very strong sources of heat arise and last for a period of hours to days. Numerous phenomena that could permit warm water to reach the surface more readily are neglected, such as bubbles or buoyant particles, or vortex rings (which trap fluid; Turner 1960), in favour of concentrating on the situation that seems to require the least special circumstances. Rise height in other geometries, such as a line source of length L or a surface flux over an area L^2, depend more strongly on the buoyancy source strength ($(F/LN^3)^{1/3}$ and $(F/L^2N^3)^{1/2}$), and might be expected to attain the surface more easily. However, to obtain these geometrical limits practically requires $L \gg H$ in which case the buoyancy source per unit length or per unit area is much reduced. In the limit $F \to \infty$ the ratio of line source penetration to point source penetration $(h_N/L)^{1/3}$ grows large since L is fixed, but for values such that $h_N \sim H$ and $L \gg H$ the line source penetration is smaller. When the ocean depth and source size are similar ($L \sim H$), details of the source geometry are likely to be important to the vertical structure of the plume. The point source model is used here only as a guide to the relation between source strength and penetration.

Weak oceanic stratification at higher latitudes obviously allows even modest hydrothermal sources to reach the surface; on the other hand the sea surface anomalies would also be modest, and moreover the air-sea interactions described above are tropical, and do not operate at higher latitudes.

To understand how a plume behaves when it encounters a thermocline it is helpful to refer to the laboratory experiment of Kumagai (1984). He studied the evolution and eventual penetration of a buoyant plume across a finite density or buoyancy jump. There is a downward buoyancy flux as the plume impinges on the interface and erodes the stratification, over a time scale which can be longer than the time scale N^{-1} implied by the above plume scaling. Relatively weak plumes can thus penetrate the thermocline, though the resulting anomaly will be weak since the plume is always near its equilibrium density. With Earth's rotation, this process might happen more readily since energy is confined; on the other hand for some parameter ranges baroclinic instability could break up the spreading plume and re-establish the thermocline stratification, prolonging or suppressing the process.

A simple plume model is used next to determine the penetration height as a function of the source strength F in the presence of a realistic thermocline. At some point the plume is buoyant enough to reach the surface. Further increases in source strength produce stronger sea surface buoyancy, or equivalently, temperature anomalies in the one component system. The spreading phase is considered in an idealized model designed to examine the tendency for Earth's rotation to confine the plume fluid, and maintain a significant anomaly in the presence of mixing. Finally, a case relevant to the release of the Red Sea hot brine reservoir is described, to highlight salinity effects.

2. An exponential thermocline

A standard plume model (Turner 1986; Little *et al.* 1987; Speer & Rona 1989) was used to find the vertical structure of the plume for a variety of source strengths. The model equations are:

$$Q_z = 2\pi RW, \tag{2.1}$$

$$M_z = \lambda^2 \pi R^2 b, \tag{2.2}$$

$$F_z = -\pi R^2 W N^2(z), \tag{2.3}$$

where W is vertical velocity, R is the radial scale for the assumed Gaussian profile. An ambient stratification N must be specified, and based on exponential fits to data from the central subtropical Pacific Ocean (similar to the Atlantic Ocean), a simple form:

$$T(z) = T_{00} + T_0 \mathrm{e}^{\delta z}, \quad S(z) = S_0, \tag{2.4}$$

appeared to be adequate to represent $N(z)$. For the runs described here, $T_{00} = 1.0$, $T_0 = 0.01$, $S_0 = 35$ for $0 \leqslant z \leqslant 2000$ m. The thickness scale $1/\delta = 250$ m. An equation relating temperature and salinity to density is required. For temperatures below 40 °C, and with S within the range of normal seawater, the full UNESCO equation of state was used. At higher temperatures Chen's (1981) result for pressure near 200 bars and constant salinity was substituted.

Initial values for Q, M and F were based essentially on the following megaplume scenario and segment scenario. From chemical and geophysical observations the megaplume was thought to form from high-temperature water venting at roughly 1 m s^{-1} along a fissure several hundred metres long, and less than 1 m wide (Baker *et al.* 1987). If the temperature were about 300 °C, typical values would be $Q = 125$ m^3 s^{-1}, $M = 62.5$ m^4 s^{-2}, $F = 50$ m^4 s^{-3}. The source F is similar to the total source strength 39 m^4 s^{-3} used by Lavelle (1995) in model studies of the megaplume (integrating over a 1200 m long line source). In the segment scenario the fissure occupies the entire segment, multiplying the total area of venting fluid by a thousand or so, and magnifying the source by a similar amount.

The standard formula for rise height $Z^* = 3.8(F/N^3)^{1/4}$ applies to a constant N or uniformly stratified environment. With arbitrary N one usually must solve numerically for the rise height (figure 1*a*); however, substituting the exponential form $N = N_0 \mathrm{e}^{\delta Z^*/2}$ and solving for Z^* turns out to give a reasonable agreement with model results (figure 1*b*). Thus the effective stratification felt by the rising plume is essentially that near the final equilibrium level. A simple approximate solution to the equation that results from the above substitution is

$$Z^* = \frac{2}{3\delta} \ln\left(\frac{F}{F_0}\right), \tag{2.5}$$

valid when the rise height is close to the full water depth, showing the logarithmic dependence This form gives heights approaching those of the plume model near the surface (figure 1*c*; $F_0 = 1$ m^4 s^{-3}).

When the strength is of order 10^4 m^4 s^{-3} the plume reaches the surface. Inertia carries the plume past its equilibrium point, though, so that it arrives at the surface with a negative buoyancy or temperature anomaly (figure 2). This would give it an appearance similar to other eddy-like structures such as the megaplume or cold-core Gulf Stream rings, with a positive upper density anomaly and negative lower density anomaly, centered on its equilibrium level.

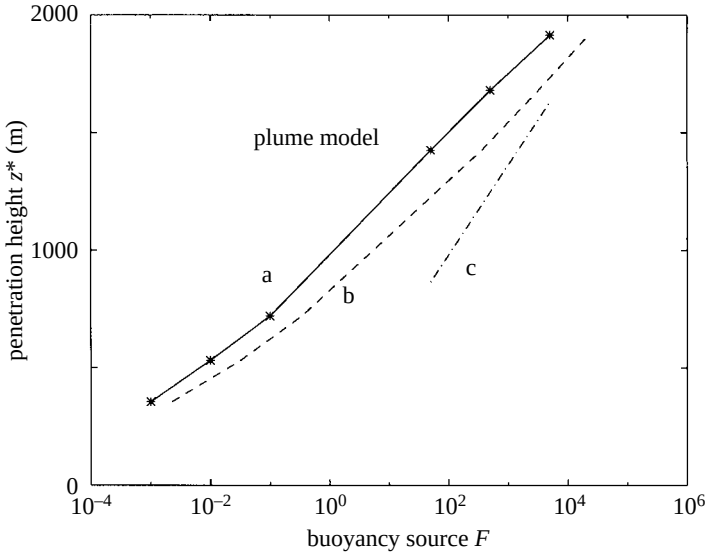

Figure 1. Plot of plume penetration height Z^* versus source strength F, results from plume model (a). Also shown are approximations based on the equation for rise height: valid for all heights (b), and simplified for heights close to the full ocean depth (c).

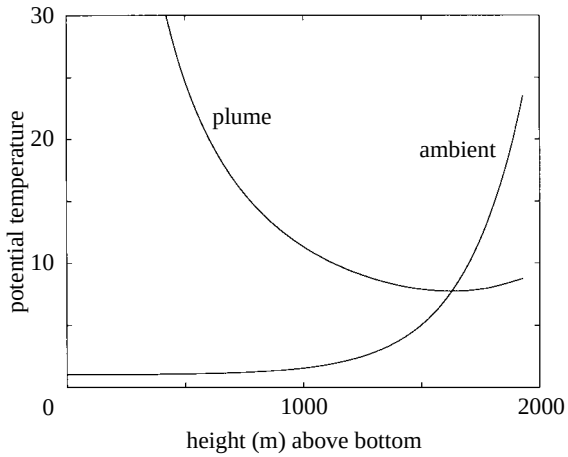

Figure 2. Plume temperature as a function of height for a source just adequate to reach the surface layer ($F = 5 \times 10^3$ m^4 s^{-3}). The initial temperature is 365 °C. The plume rises at about 5 m s^{-1} over most of the water column. Also shown is the exponential ambient temperature representing the thermocline. The top of the plume is cool relative to ambient surface water.

Of particular interest is the possibility that the plume could raise the sea surface temperature. Increasing the source strength raises the centreline temperature to surface values at about $F = 3 \times 10^5$ m^4 s^{-3} (figure 3). Beyond this point, SST rises slowly, as expected from plume scaling for buoyancy, giving rise to anomalies of several degrees. At values of 6×10^6 m^4 s^{-3} the SST is potentially high enough to have important local air–sea interaction effects (e.g. Emanuel *et al.* 1995). However, such effects are only plausible if the anomaly covers a significant area of the ocean, larger than that of the plume, and if it lasts for a period of time sufficient for the

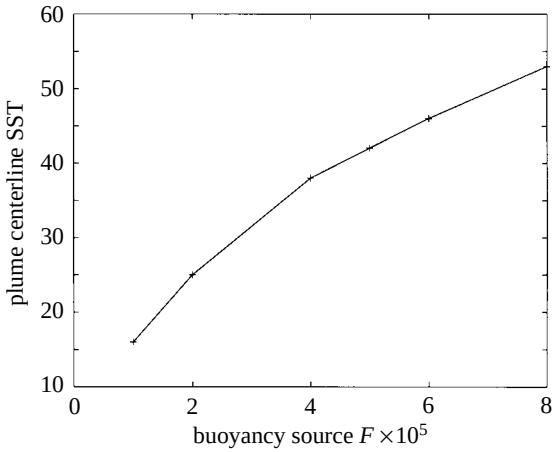

Figure 3. Plume temperature at the surface for various source strengths ($m^4\ s^{-3}$). The ambient SST is about 30 °C. Only sources stronger than about $3 \times 10^5\ m^4\ s^{-3}$ actually raise SST for the present choice of thermocline structure.

atmosphere to react, of the order of one day. A simple model of the spreading phase is presented next to address these issues.

3. A circular slab model of spreading

The time evolution of lenses of fluid, either stratified or homogeneous, is the subject of much research; in different contexts they are commonly observed in the ocean, and their dynamics includes many interesting processes (McWilliams 1985). Here, a drastically simplified set of equations is obtained by focusing on bulk balances in a circular slab, and the evolution of its perimeter.

The plume fluid is assumed to spread out on the surface axisymmetrically to radius R, in a layer with mean thickness h and buoyancy g' (figure 4). The surrounding water has a constant density and zero buoyancy. Conservation of mass or volume $V_{OL} = \pi R^2 h$ gives, in the presence of mixing represented by a vertical entrainment velocity W_e (see later):

$$\frac{dV_{OL}}{dt} = Q + W_e \pi R^2, \tag{3.1}$$

with Q the amount of plume fluid feeding the slab.

The equation for the bulk balance of buoyancy in the slab is

$$\frac{d(g' V_{OL})}{dt} = Q g'_0, \tag{3.2}$$

where g'_0 is the buoyancy of the entering plume fluid.

A reduced-gravity model with motion only in the buoyant layer is commonly used in the study of fronts and vortices (e.g. Cushman-Roisin *et al.* 1985). Often, strong assumptions about the spatial structure of the vortex are made to simplify the problem. Here, we ignore the spatial structure completely and focus on the evolution of the rim, or radius R. The specification of the pressure gradient at the rim, which normally involves the spatial structure, is contrived to produce a simplified set of equations that mimic the behaviour of the more complicated model. The equations of motion of a parcel at R, together with bulk mass and buoyancy conservation, are

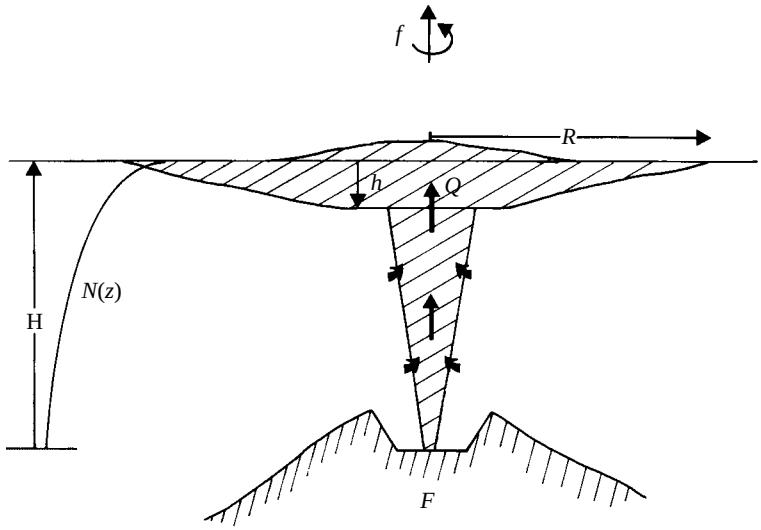

Figure 4. Schematic of a plume resulting from a major eruption on a ridge. The plume rises through a thermocline $N(z)$ and spreads out laterally on the surface, with a continuous supply Q of fluid from below.

written as:

$$\dot{R} = u,$$
$$\dot{u} = g'h/R + fv - \frac{W_e}{h}u + \frac{v^2}{R},$$
$$\dot{v} = -fu - \frac{W_e}{h}v - \frac{uv}{R},$$
$$\dot{h} = \frac{Q - 2\pi Rhu}{\pi R^2} + W_e,$$
$$\dot{g}' = \frac{Q}{V_{OL}}(g'_0 - g') - \frac{W_e}{h}g'.$$

All radial structure is ignored, and the radial pressure gradient has been replaced by the form $g'h/R$, simulating the hydraulic pressure drop across the rim, of reduced amplitude at large radius or small thickness. These simplifications eliminate many processes, including wave radiation, but the primary interest here is the effect of mixing. Exact particular solutions to *inviscid* equations for the time-dependent motion of a lens of fluid at the surface were obtained by Cushman–Roisin *et al.* (1985), showing the basic modes of motion of circular and elliptic vortices. In the above system, a mixing term in the form of a vertical entrainment velocity is included:

$$W_e = E_0\, Ri^{-1}\, s, \quad s = \sqrt{u^2 + v^2}, \tag{3.3}$$

parametrized here as a function of a Richardson number $Ri = g'h/s^2$, which is small (and mixing large) when the scale for inertial forces is stronger than that for buoyancy forces (Turner 1986). Values for E_0 are zero (no mixing) or 10^{-3}. This parametrization is meant only to capture roughly the changes in properties due to mixing with the surrounding water as the plume spreads.

Initial conditions are set at a radius $R_0 = 5000$ m, by which point the plume's radial expansion has decreased to values more appropriate for the above system.

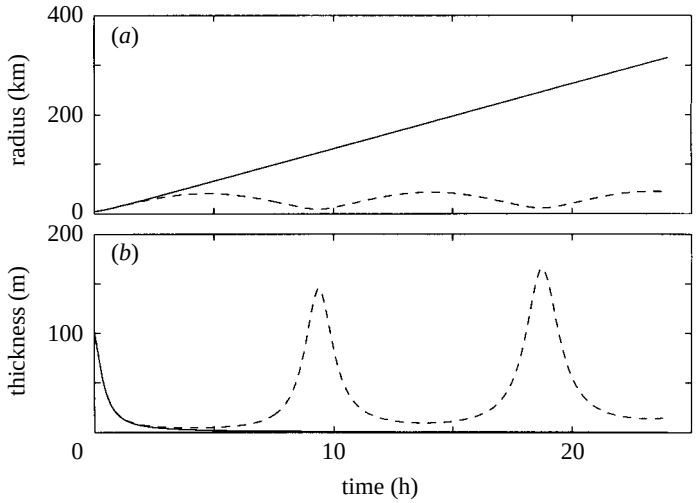

Figure 5. Slab model solutions without mixing. Radius versus time (upper panel) without rotation (solid), and with rotation (dashed). Thickness versus time (lower panel) without (solid) and with (dashed) rotation.

They are: $h = 100\,\mathrm{m}$, $g' = 0.1\,\mathrm{m\,s^{-2}}$, $u = 1\,\mathrm{m\,s^{-1}} \sim \sqrt{g'h}$, and $v = 0$. The other parameters are $f = 10^{-4}\,\mathrm{s^{-1}}$ and $Q = 10^6\,\mathrm{m^3\,s^{-1}}$. Starting at smaller radii and higher velocity exaggerates the behaviour described here, but does not produce new behaviour. Initial thickness was chosen arbitrarily; initial buoyancy corresponds to a temperature anomaly of tens of degrees. The radial velocity for small time is $g'ht/R_0$, and it increases to values *ca.* $\sqrt{g'h}$ if the slab starts from rest.

Overall, the magnitude of the (specific) angular momentum for a circular disk $L = V_{OL}Rv/2$ increases owing to lateral expansion and Earth's rotation, spinning up anticyclonic motion in the slab, similar to the case for normal nonbuoyant hydrothermal lenses (Lavelle & Baker 1994; Speer & Marshall 1995). The centrifugal force term v^2/R plays a small role and u and v are basically out of phase. Note that the slab can regain buoyancy lost to mixing, since the plume resupplies it at the initial value g'_0.

Solutions with no mixing show the basic behaviour with and without rotation (figure 5). Without rotation the slab expands and thins monotonically; with rotation, the expansion is arrested after one quarter of an inertial period ($2\pi/f$), and the plume begins to pulsate. A similar pulsation of a circular lens was described by Cushman–Roisin *et al.* (1985). Thickness grows rapidly near the minimum radius owing both to contraction and filling (Q).

Ignoring the nonlinear velocity terms and mixing, the equations for u and v can be combined into one equation:

$$\ddot{u} + f^2(1 + (3R_\mathrm{d}^2/R^2))u = 0, \tag{3.4}$$

$$R_d^2 = g'h/f^2, \tag{3.5}$$

where R_d is the deformation radius. Substituting $u = u_0 \mathrm{e}^{\mathrm{i}\omega t}$ gives $\omega^2 = f^2(1 + 3R_\mathrm{d}^2/R^2)^{1/2}$ showing free oscillations analogous to Poincaré waves, for which $\omega^2 = f^2 + \kappa_\mathrm{H}^2 gH$, where κ_H is the horizontal wavenumber. For g' and f as above, and with $h = 10\,\mathrm{m}$ at $R = 25\,\mathrm{km}$, the frequency is about $1.2f$. In the linear, horizontally uniform limit ($R \to \infty$) the effect of mixing is only to dampen the oscillations, and

not to modify their frequency; solutions with and without mixing tended to show a spectral peak near $1.5f$, qualitatively consistent with the linear limit.

The damping effect is illustrated in solutions with mixing (figure 6). The initial pulsation period has increased by about 25%, measured by the time to the first thickness maximum, but further oscillations are only about 10% slower than the case without mixing. Velocities (figure 6*b*) show the adjustment to geostrophic-like flow with negative azimuthal flow v, and radial velocity oscillating about zero. Froude number $Fr = \sqrt{Ri^{-1}}$ is a gauge of mixing since it is large when mixing is large. Rotation tends to diminish mixing by preserving thickness. In these solutions, the Burger number R_d/R rapidly approaches a value of roughly 0.5, passing through a minimum near $tf \sim 3$, but remaining close to 0.5 for longer times. Finally, a key result is the stronger buoyancy or temperature anomaly with rotation. Confinement and reduced mixing allows the central plume to recharge the surface layer and maintain buoyancy. There is little dissipation even after 100 h (figure 7). By this time ($tf \sim 10$–100) baroclinic instability is likely to be developing, causing a horizontal displacement of the entire slab away from the source (Helfrich & Speer 1995).

4. A Red Sea brine plume

At the bottom of the Red Sea, pools of hot brine have been formed by the exchange of heat and chemicals between seawater and the seafloor, with temperatures above 60 °C and salinities of roughly 250‰ (Ross 1983), giving a density of about 1200 kg m^{-3}. The overlying deep water, at 22 °C and 40.5‰, has a density close to 1030 kg m^{-3}. To make the dense brine buoyant, its temperature must be raised several hundred degrees by volcanic activity.

The standard plume equations were modified to deal with heat and salinity transports separately:

$$H_z = -\lambda_f^{-1}\rho_0 C_p Q \frac{\partial T_\mathrm{amb}}{\partial z}, \tag{4.1}$$

$$S_z = -\lambda_f^{-1}\rho_0 Q \frac{\partial S_\mathrm{amb}}{\partial z} 10^{-3}, \tag{4.2}$$

where $H = \lambda_f^{-1}\rho_0 C_p Q(T - T_\mathrm{amb})$, $S = \lambda_f^{-1}\rho_0 Q(S - S_\mathrm{amb})$ and $\lambda_f^{-1} = (1+\lambda^2)/\lambda^2$. Now the buoyancy transport $F = \lambda_f^{-1} Q b$, with b calculated from an equation of state. Salinity was accomodated in the simplest possible way at high temperature by setting the haline contraction coefficient $\beta = 0.9 \times 10^{-3}$ for $T > 40$ °C. The resulting potential density (figure 8) has curvature due to the temperature dependence alone.

This diagram helps to illustrate how dense brine might become buoyant. All water to the right of about 1028.5 kg m^{-3}, the density of the bottom water, is nonbuoyant. Heating, to increase temperature, or mixing with overlying water, to reduce salinity, is required to generate a buoyant plume. Thus dense brine in the lower right-hand part of the diagram migrates up (with heating) and to the left (with mixing) to become finally buoyant. Then it rises off the seafloor and entrains the fluid surrounding it. To represent this entrainment temperature and salinity profiles were chosen to simulate the Red Sea (figure 9). Only a finite volume on the order of several cubic kilometres of brine is available at the source; the vertical transport in the plume drains this volume in a period of hours to days (table 3).

Two solutions are plotted (figure 10) in order to make two points. The first is that if the buoyancy source is strong enough, then the plume can reach the surface

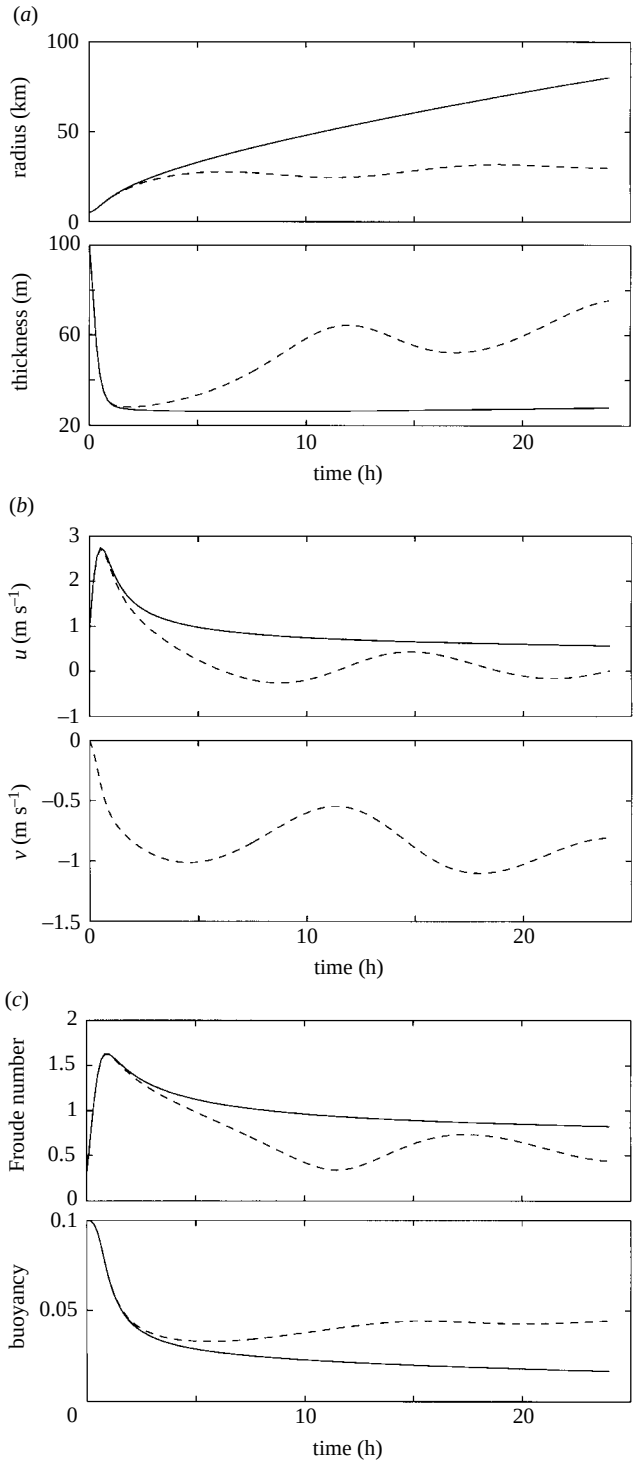

Figure 6. Slab model solutions with mixing. (*a*) Radius (upper) and thickness (lower) without rotation (solid), and with rotation (dashed). (*b*) Radial (upper) and azimuthal (lower) velocity. Azimuthal velocity is zero without rotation. (*c*) Froude number (upper) and buoyancy (lower).

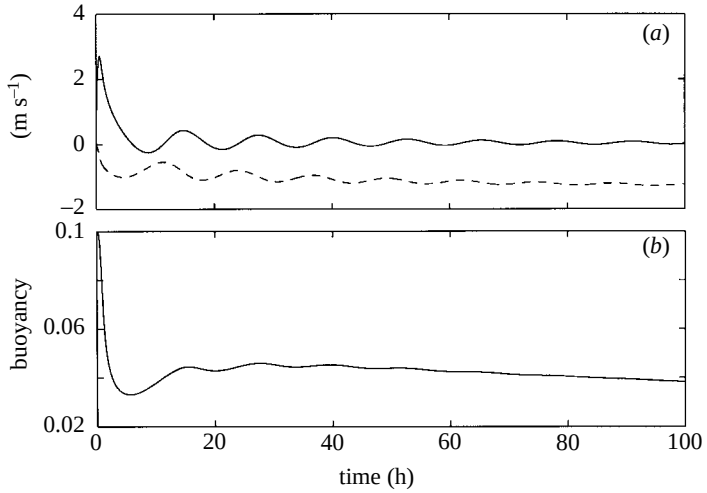

Figure 7. Longer slab model run with rotation. Upper panel shows radial (solid) and azimuthal (dashed) velocity; lower panel shows nearly constant buoyancy after one day.

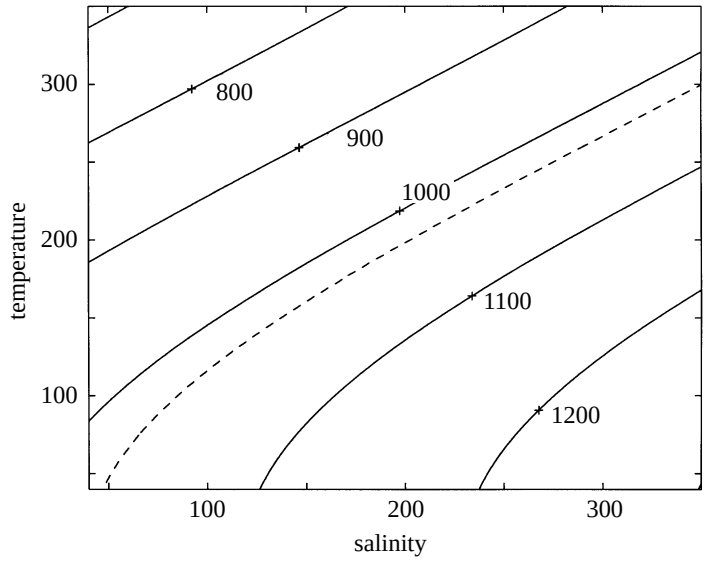

Figure 8. Density (kg m^{-3}) from a simplified high temperature and salinity equation of state. Bottom density (dashed) separates buoyant from nonbuoyant source conditions. Note that on this scale, the full density range (1024–1028.5 kg m^{-3}) of the idealized Red Sea lies nearly along the curve for bottom density.

as before. Here, in order to be that strong, it seems to be necessary to reduce the salinity of the brine quite substantially. Presumably the motion generated by any major eruption could do so by stirring up water near the seafloor. Second, mixing between the rising plume and the interior or ambient seawater drives T and S toward ambient values, but because of the curved isopycnals, the *density* of the plume can become equal to that of the surrounding water at some intermediate level. This cabelling effect (Sato 1972) halts the plume at mid-depth, despite the absence of any stratification ($N_T = N_S = N = 0$) at these levels. Subsequent turbulent mixing is reduced as a lens is formed, isolating a core of the plume fluid from its surroundings.

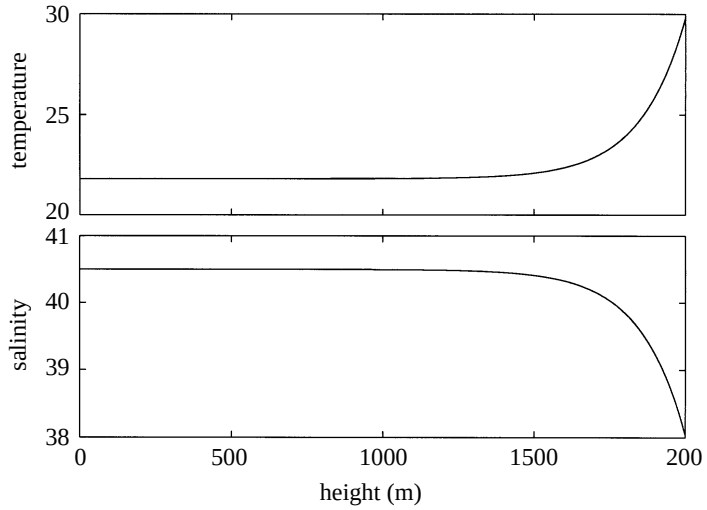

Figure 9. Idealized ambient temperature and salinity versus height for the Red Sea.

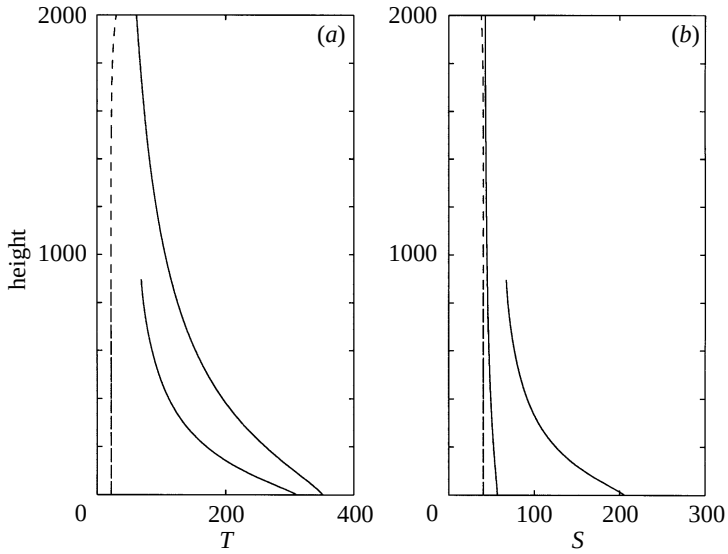

Figure 10. Plume solutions for the Red Sea case with ambient structure (dashed). The plume starting at higher temperature and lower salinity reaches the surface; another plume reaches its equilibrium level at mid-depth.

Table 3. *Source conditions for Red Sea runs*

penetration	$\mathcal{H}$ (MW)	$\mathcal{S}$ (kg s^{-1})	F (m^4 s^{-3})	Q (m^3 s^{-1})	T (°C), S (‰)
surface	8×10^8	1×10^7	1.9×10^6	1×10^6	350, 57
mid-depth	7×10^7	1×10^7	8×10^4	1×10^5	309, 205

5. Discussion

Buoyant plumes generated by geothermal sources typically rise in a stratified environment, ultimately due to solar heating or chemical components in oceans, lakes

and atmospheres. Only a single case among the tremendous variety of possibilities has been investigated here, to focus on what appears to be a ubiquitous problem: plume penetration through a thermocline, or more generally, a pycnocline. Many other phenomena such as seamount volcanism or air–sea interaction are capable of modifying the surface layer properties of the ocean as well, without the burden of crossing a thermocline.

Some aspects of the solutions presented here apply more generally to hydrothermal plumes, such as the expected oscillation of the lens, and a possible two-component mixing behaviour. An interesting area for future study is the initial supercritical expansion of the plume fluid, whether on the surface or internally, as it spreads laterally. Also, two-component effects, such as double diffusion, with a broad definition of salinity to include diverse chemical compositions, might turn out to be quite relevant to normal hydrothermal plumes, which tend to create T–S anomalies by their nature (see also Campbell *et al.* 1984). The complicated chemical mixture that makes up some geothermal sources could add new effects to plume dynamics; thus far, however, promising avenues for such effects seem to be the generation of vapour and brine phases, thought now to be a rather generic aspect of ridge systems, as well as the release of bubbles in shallow seafloor systems.

The very large transfer of heat required to create thermocline-penetrating plumes must make them rare events. The circumstances of the eruption process leading, moreover, to such transfers remains unclear. Studies of heat transfer in shallow underwater eruptions might be feasible and helpful in this regard. At a fundamental level, it is the rate of heat exchange that drives hydrothermal circulation, whether this takes the form of rising plumes or slow seepage through porous crust. Better constraints on heat flow or the circulation driven by it at any length and time scale are valuable.

Support is provided by the CNRS. The international RIDGE community supports a forum for interesting interdisciplinary exchanges, from which I have benefited. K. Emanuel restimulated interest in getting a plume to the surface, and the Royal Society generously provided the occasion; thoughtful comment on the subject from K. Helfrich is appreciated.

References

Baker, E. T., Massoth, G. J. & Feely, R. A. 1987. Cataclysmic hydrothermal venting on the Juan de Fuca Ridge. *Nature* **329**, 149–171.

Campbell, I. H., McDougall, T. J. & Turner, J. S. 1984 A note on the fluid dynamic processes which can influence the deposition of massive sulfides. *Econ. Geol.* **79**, 1905–1913.

Chen, C.-T. A. 1981 Geothermal systems at 21° N. *Science* **211**, 298.

Cushman-Roisin, B., Heil, W. H. & Nof, D. 1985 Oscillations and rotations of elliptical warm-core rings. *J. Geophys. Res.* **90**, 11 756–11 764.

Emanuel, K. A., Speer, K.,Rotunno, R., Srivastava, R. & Molina, M. 1995 Hypercanes: a possible link in global extinction scenarios. *J. Geophys. Res.* **100**, 13 755–13 765.

Helfrich, K. R. & Speer, K. G. 1995 Oceanic hydrothermal circulation: mesoscale and basin-scale flow. In *Seafloor hydrothermal systems, physical, chemical, biological and geological interactions* (ed. S. Humphries, R. Zierenberg, L. Mullineaux & R. Thomson), pp. 347–356. Geophysical Monograph 91, American Geophysical Union.

Kumagai, M. 1984 Turbulent buoyant convection from a source in a confined two-layered region. *J. Fluid Mech.* **147**, 105–131.

Lavelle, J. W. 1995 The initial rise of a hydrothermal plume from a line segment source: results from a three-dimensional numerical model. *Geophys. Res. Lett.* **22**, 159–162.

Lavelle, J. W. & Baker, E. T. 1994 A numerical study of local convection in the benthic ocean induced by episodic hydrothermal discharges. *J. Geophys. Res.* **99**, 16 065–16 080.

Little, S. A., Stolzenbach, K. D. & Von Herzen, R. P. 1987. Measurements of plume flow from a hydrothermal vent field. *J. Geophys. Res.* **92**, 2587–2596.

McWilliams, J. C. 1985 Submesoscale, coherent vortices in the ocean. *Rev. Geophys.* **23**, 165–182.

Ross, D. A. 1983 The Red Sea. In *Estuaries and enclosed seas* (ed. B. H. Ketchum), pp. 293–307. Amsterdam: Elsevier.

Sato, T. 1972 Behaviours of ore-forming solutions in seawater. *Mining Geol.* **22**, 31–42.

Speer, K. G. & Marshall, J. 1995 The growth of convective plumes at seafloor hot springs. *J. Mar. Res* **53**, 1025–1057.

Speer, K. G. & Rona, P. A. 1989 A model of an Atlantic and Pacific hydrothermal plume. *J. Geophys. Res.* **94**, 6213–6220.

Turner, J. S. 1960 A comparison between buoyant vortex rings and vortex pairs. *J. Fluid Mech.* **33**, 639–656.

Turner, J. S. 1986 Turbulent entrainment: the development of the entrainment assumption and its application to geophysical flows. *J. Fluid Mech.* **173**, 431–471.

Walker, D. 1995 More evidence indicates links between El Niños and seismicity. *EOS Transactions*, vol. 76. Washington, DC: American Geophysical Union.

Wilson, L., Sparks, R. S. J., Huang, T. C. & Watkins, N. D. 1978 The control of eruption column heights by eruption energetics and dynamics. *J. Geophys. Res.* **83**, 1829–1836.

Discussion

D. A. Rothery (*Department of Earth Sciences, The Open University, Milton Keynes, UK*). In the case of a plume capable of reaching the surface, what would be the possible effects of currents encountered at different depths (i) during initial uprise, and (ii) throughout the lifetime of the plume? For (ii) I am wondering in particular to what extent surface currents could upset your simple model of a plume head spreading out at the surface, and rotating so as to conserve vorticity. I would expect most plume heads to be transported laterally by surface currents, so a simple disc-like rotating head seems unlikely.

K. G. Speer. During the initial rise, and within a few thousand metres of the origin of the plume on the surface, velocity scales are greater than 1 m s^{-1}. This is larger than typical maximum ocean current speeds, and they would therefore be expected to have little effect. After a day or so, strong ocean currents, if present, could very well distort the plume substantially as suggested; nevertheless, the rotational constraint still tends to keep the plume from spreading without limit under gravity.

D. Pyle (*Department of Earth Sciences, University of Cambridge, UK*). Cooling of 1 kg of basalt releases about 1.5 MJ. To sustain the heat-fluxes needed to drive these model megaplumes requires an eruption of 10^4–10^5 m^3 of magma per second. This is an unreasonably large flux for a point source eruption. During a rift eruption, it might be possible to sustain a flux of up to 1–10 m^3 s^{-1} of magma per metre length of fissure, requiring a fissure source up to tens of kilometres long. Could ? Speer comment on the difference that a sustained line source, rather than point source, might make to his model?

K. G. Speer. A line source whose length scale is similar to rise height will probably have similar overall behaviour, though different detailed structure. Scaling presented

in the text suggest that line sources of this size are more effective and more plausible sources, and a rift or segment scenario was envisioned. Constraints of the sort offered on magma flux are helpful in determining the geophysical possibility of this phenomenon, independent of its oceanographic consequences.

PHILOSOPHICAL TRANSACTIONS OF THE ROYAL SOCIETY A MATHEMATICAL, PHYSICAL & ENGINEERING SCIENCES